Journal of Power Sources 416 (2019) 56–61

Contents lists available at ScienceDirect

Journal of Power Sources

journal homepage: www.elsevier.com/locate/jpowsour

Bottom-current-collector-free thin-film batteries using $LiNi_{0.8}Co_{0.2}O_2$ epitaxial thin films

Kazunori Nishio[a,*], Koji Horiba[b], Naoto Nakamura[a], Miho Kitamura[b], Hiroshi Kumigashira[b,c], Ryota Shimizu[a,d], Taro Hitosugi[a]

[a] School of Materials and Chemical Technology, Tokyo Institute of Technology, Tokyo, 152-8552, Japan
[b] Photon Factory, Institute of Materials Structure Science, High Energy Accelerator Research Organization (KEK), Tsukuba, 305-0801, Japan
[c] Institute of Multidisciplinary Research for Advanced Materials, Tohoku University, Sendai, 980-8577, Japan
[d] Japan Science and Technology Agency, Presto, Saitama, 332-0012, Japan

HIGHLIGHTS

- Bottom-current-collector-free 4-V-class thin film lithium batteries are fabricated.
- $LiNi_{0.8}Co_{0.2}O_2$ is selected because of high electrical conductivity.
- A very flat $LiNi_{0.8}Co_{0.2}O_2$ surface with a roughness of 0.44 nm was obtained.
- $LiNi_{0.8}Co_{0.2}O_2$ thin-film batteries exhibit stable operation.

GRAPHICAL ABSTRACT

A top-view picture (Left) and schematic cross section (Center) of a fabricated thin-film lithium batteries using $LiNi_{0.8}Co_{0.2}O_2$ epitaxial thin films. Right: Schematic side view of lithium-ion conduction across the interface between $LiNi_{0.8}Co_{0.2}O_2$ and Li_3PO_4.

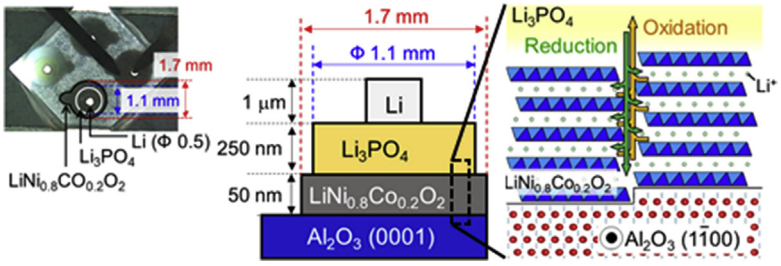

ARTICLE INFO

Keywords:
Solid-state battery
$LiNi_{0.8}Co_{0.2}O_2$
Epitaxial thin film
Pulsed laser deposition
Interface resistance

ABSTRACT

The decrease in the resistance at solid electrolyte and electrode interfaces has become a critical issue in the development of solid-state lithium batteries. To understand the ionic transport properties across solid electrolyte and electrode interfaces, thin-film batteries consisting of flat epitaxial films are of considerable importance. Herein, we report the operation of bottom-current-collector-free thin-film batteries using $LiNi_{0.8}Co_{0.2}O_2$ epitaxial thin films. As the bottom current collector is not inserted between the substrates and $LiNi_{0.8}Co_{0.2}O_2$, the surface of $LiNi_{0.8}Co_{0.2}O_2$ is very flat, with a surface roughness average of approximately 0.44 nm. This study proposes a very flat electrode surface suitable for the investigation of interfacial phenomena at solid electrolyte and electrode interfaces.

1. Introduction

Solid-state lithium batteries are promising candidates for energy storage devices because of their potential for enhanced safety and high energy density [1,2]. However, the batteries have faced the drawback of a low power density originating from the high resistance at solid electrolyte and electrode interfaces. Accordingly, decreasing the interface resistance has become a critical issue. Indeed, interface resistance has been reduced by inserting buffer layers between sulfide electrolytes and $LiCoO_2$ [3]; however, the reduction of the interface resistance remains unsatisfactory. The understanding and control of interface resistance remains inadequate despite the importance of fabricating low-

* Corresponding author.
E-mail address: nishio.k.ag@m.titech.ac.jp (K. Nishio).

https://doi.org/10.1016/j.jpowsour.2019.01.067
Received 7 November 2018; Received in revised form 16 January 2019; Accepted 23 January 2019
0378-7753/

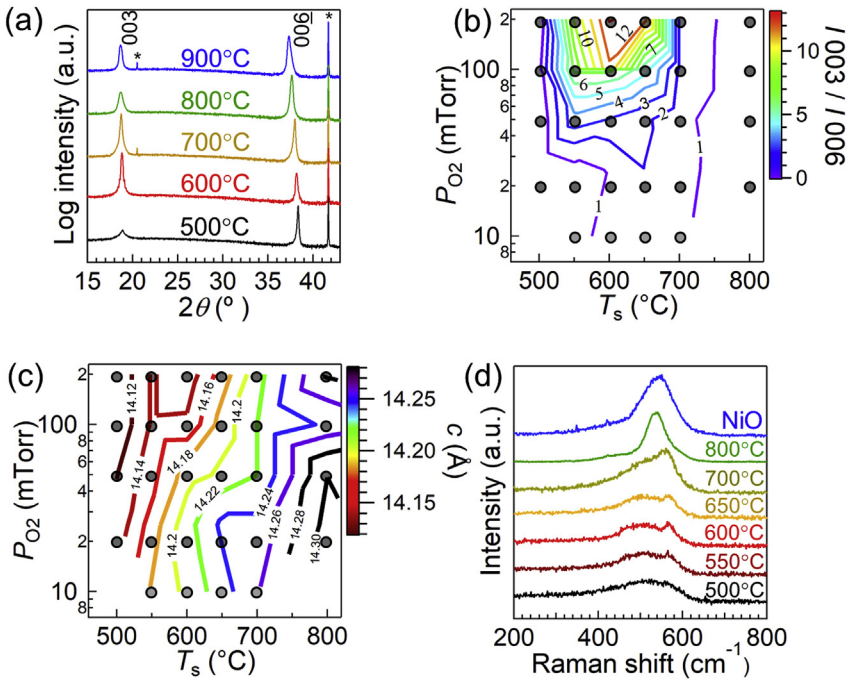

Fig. 1. (a) Out-of-plane X-ray diffraction patterns for the $LiNi_{0.8}Co_{0.2}O_2$ (LNC) thin films grown at a variety of substrate temperatures (T_s) (oxygen partial pressure, P_{O2}, of 100 mTorr). Asterisks indicate the diffractions from the Al_2O_3 substrate. (b) Intensity ratio mapping of 003–006 peaks (I_{003}/I_{006}). (c) *c*-axis lattice constant for LNC thin films grown at a variety of T_s (from 500 to 800 °C) and P_{O2} (from 10 to 200 mTorr). Gray circles in (b) and (c) indicate the thin films fabricated in this study. (d) Raman spectra of the LNC thin films (thickness of ~80 nm) grown at a variety of T_s (P_{O2} = 100 mTorr). The blue plot indicates the spectrum of a rock-salt-type NiO thin film on Al_2O_3 (0001).

resistance interfaces.

One approach for understanding the origin of interface resistance, namely, understanding the ionic transport properties across solid-electrolyte/electrode interfaces, is to use thin-film batteries consisting of epitaxial films. This approach provides well-defined interface atomic structures, surface areas, and crystal orientations, enabling quantitative evaluation of interface resistance. We have reported an extremely low interface resistance in $LiCoO_2/Li_3PO_{4-x}N_x$ and $LiNi_{0.5}Mn_{1.5}O_4/Li_3PO_4$ thin-film batteries and demonstrated fast charging capabilities [4,5]. To further investigate interfacial properties, a flat, positive electrode surface is desired. However, the roughness of the bottom electrode (metal current collector), inserted between the positive electrodes and substrates, hinders the achievement of flatter and better-controlled electrode surfaces. Accordingly, to eliminate the bottom current collector, depositions of highly electronically conducting positive-electrode materials are extremely important.

Herein, we report the growth of high-quality $LiNi_{0.8}Co_{0.2}O_2$ (LNC) epitaxial thin films using pulsed laser deposition (PLD) and demonstrate the operation of a bottom-current-collector-free solid-state battery. LNC is one of the most electrically conductive materials among positive-electrode materials [6]; accordingly, we demonstrate the operation of bottom-current-collector-free thin-film batteries. Films deposited on Al_2O_3(0001) substrates exhibit a surface roughness average (R_a) of 0.44 nm. The resulting thin-film batteries using the epitaxial thin films show very stable battery properties with a low solid-electrolyte/electrode interface resistance. These results open opportunities for preparing an ideal, atomically flat model electrode suitable for investigating ionic transport across electrolyte/electrode interfaces.

2. Experiment

2.1. Fabrication of $LiNi_{0.8}Co_{0.2}O_2$ epitaxial thin films

We used PLD to fabricate LNC epitaxial thin films. The details of the PLD system were reported previously [7–9]. We employed a KrF excimer laser (wavelength 248 nm, pulse duration ~20 ns) operated at 5 Hz to ablate a $Li_{1.3}Ni_{0.8}Co_{0.2}O_{2+\delta}$ target (Toshima Manufacturing Co., Ltd.). Note that we increased the Li content by 30% to compensate for the loss of Li during deposition. The typical spot size and laser pulse fluence at the target surface were 0.019 cm^2 and 1.39 J/cm^2, respectively. The laser intensity during growth was measured before deposition [10]. The target–substrate distance was ~47 mm. Thin films were deposited onto Al_2O_3 (0001) substrates with a step-and-terrace surface (5 × 5 cm^2 and 0.5 mm in thickness) prepared by annealing the substrates at 1000 °C for 3 h in air. Substrate temperatures (T_s) and oxygen partial pressures (P_{O2}) during LNC thin-film growths were varied from 500 to 900 °C and 10–200 mTorr, respectively.

2.2. Characterization of $LiNi_{0.8}Co_{0.2}O_2$ epitaxial thin films

The structural properties of the thin films were characterized by X-ray diffraction (XRD) (Bruker D8 DISCOVER). The thin film qualities were evaluated using a Raman spectrometer with a 532-nm excitation line (NRS-4100, Jasco Corp.), Rutherford backscattering spectroscopy (RBS), and particle-induced X-ray emission (PIXE). The oxidation states of Ni and Co inside the LNC thin films were measured using X-ray absorption spectroscopy (XAS) in the total electron yield (TEY) mode using the sample drain current (surface-sensitive mode) and transmission mode using X-ray excited optical luminescence from the Al_2O_3 substrates (bulk-sensitive mode) at the beamline BL-2A MUSASHI of Photon Factory, KEK. The samples were exposed to air during their transfer to the beamline. Co L_3 edge spectra and Ni L_3 edge spectra were scaled to the peaks at 780 eV and shoulder structures at ~855 eV, respectively.

2.3. Fabrication and characterization of thin-film battery

For demonstrating battery performance, all the processes including the fabrication and electrochemical characterization of the thin-film battery were carried out using an all-in-vacuum fabrication and evaluation system [7]. The solid-electrolyte Li_3PO_4 thin film was deposited on the LNC thin film at room temperature via PLD with an ArF excimer laser (wavelength of 193 nm). A lithium-metal thin film was deposited on the electrolyte via conventional thermal evaporation. Details regarding the deposition of Li_3PO_4 and lithium are described in earlier reports [7,11].

3. Results and discussion

First, we discuss the growth of epitaxial thin films. Fig. 1(a) shows the T_s-dependent structures of films deposited at P_{O2} = 100 mTorr. Out-of-plane XRD patterns of the films deposited at T_s = 500–900 °C showed peaks similar to the 003 and 006 peaks of LNC (layered rock-salt α-$NaFeO_2$ structure ($R\bar{3}m$)). Here, we temporarily assign the peaks at ~18.81 and ~38.17° as LNC 003 and 006, respectively. Notably, the intensity of the 003 and 006 peaks strongly depended on T_s, and the films deposited at T_s = 600 and 700 °C showed sharp peaks.

To further optimize growth conditions, thin films were prepared at a variety of T_s and P_{O2} in the ranges of 500–900 °C and 10–200 mTorr, respectively. We first focus on the peak intensity ratio of 003 and 006, I_{003}/I_{006}, which is a measure of crystallinity. The α-$NaFeO_2$ type LiMO_2 (M represents transition metals such as Co and Ni) structures have highly ordered cation sublattices in which Li and M ions occupy alternating {111} layers of octahedral sites. The film quality degrades when M ions occupy Li sites and vice versa; this disordering of Li and M ions accompanies a transformation to the rock-salt-like structure [12,13]. Accordingly, the I_{003}/I_{006} values are a measure of cation ordering; a larger value indicates greater ordering. Fig. 1(b) summarizes the P_{O2} and T_s dependence of I_{003}/I_{006} values. The values are the largest in films deposited in the regions that satisfy T_s = 600–650 °C and $P_{O2} \geq$ 100 mTorr.

Next, we focus on the c-axis lattice parameter, which is also a measure of crystallinity. Fig. 1(c) shows the c-axis lattice parameters depending on P_{O2} and T_s. The region between c = 14.16 Å (red curve) and 14.18 Å (orange curve) shows the c-axis lattice parameter similar to that of the bulk reference, 14.1689 Å [12]. The increase in T_s led to the monotonic increase in the c-lattice parameters for all P_{O2}. These results could be interpreted as the formation of oxygen deficiencies in the LNC thin films [14]. Moreover, such reductions presumably induced cation disordering owing to the similar ionic radii of Li^+ (0.74 Å) and Ni^{2+} (0.69 Å); this is supported by the decrease in I_{003}/I_{006} values with an increasing T_s [15].

We further measured Raman spectra to investigate the presence of impurity phases [Fig. 1(d)]. The samples deposited at T_s below 700 °C exhibited strong LNC signatures. The sharp peak at 560 cm^{-1} and broad peak ranging from 430 cm^{-1} to 550 cm^{-1} were attributable to the A_{1g} and E_g modes of the layered rock-salt structure ($R\bar{3}m$), respectively, similar to the case for the LNC bulk reference [16]. We observed no impurity phases such as Co_3O_4 or NiO. In contrast, the thin film grown at T_s = 800 °C exhibited a single peak at 536 cm^{-1}, strongly suggesting the growth of a rock-salt-structure LNC ($Fm3m$) [17].

Considering the I_{003}/I_{006} values, c-axis lattice parameters, and Raman spectra, the best-quality LNC thin film was obtained at T_s = 600 °C and P_{O2} = 100 mTorr. For the films deposited at this condition, we observed a Laue fringe around the LNC 003 reflection [Fig. 2(a)] and the full width at half maximum of the rocking curve for the 003 reflection was 0.0961° [Fig. 2(b)]. Fig. 2(c) exhibits the in-plane XRD pattern along the Al_2O_3 [10–10] direction. The a-axis lattice constant evaluated from the LNC 110 peak was 0.287 nm, which is in good agreement with that of the bulk reference (0.28676 nm) [12].

The films had two domains rotated by 60° along the c-axis. Fig. 2(d) shows azimuthal ϕ scans for LNC 113, LNC 104, and the Al_2O_3 11–23 diffraction. The six-fold symmetry indicates that two types of domains rotated by 60° were formed in the films. The in-plane epitaxial relationships were Al_2O_3(10-10)IILNC(2–10) and Al_2O_3(10-10)IILNC(110) for each domain. Similar domain structures were observed as the anti-phase domains for a c-axis-oriented $LiCoO_2$ epitaxial thin film on the step-and-terrace surface of Al_2O_3(0001), with a typical size of 100–1000 nm depending on the terrace width of the substrate [18,19]. The surface roughness average R_a of a 50-nm-thick LNC thin film was ~0.44 nm over 2 × 2 μm^2 (Fig. 2(e)). This value is much smaller than that of the $LiCoO_2$ thin films with Au bottom current collectors reported in an earlier study (R_a ~2.5 nm) [4].

We next investigated the transition metal composition for the best-quality LNC thin film using RBS and PIXE and confirmed that the film composition was $LiN_{0.8}Co_{0.2}O_2$. Fig. S1(a) shows the energy spectrum of backscattered ions for the approximately 250-nm-thick LNC thin film along with the simulated spectrum for a 250-nm-thick LNC thin film. Although the composition of Ni and Co could not be evaluated directly using RBS because of the very similar atomic weights of Ni and Co, the compositions of both Ni and Co were resolved using PIXE. Fig. S1(b) exhibits the measured PIXE spectra along with the simulation results. The results showed that the Co/Ni ratio was 0.26 ± 0.05, indicating that the film composition was $LiNi_{0.8}Co_{0.2}O_2$, as expected from the target composition. Furthermore, the results indicated that Ni and Co were distributed homogeneously in the films (Fig. S1(c)).

We now discuss the oxidation states. As high-temperature deposition often leads to the formation of lower valence states, controlling oxidation states of Ni and Co is crucial in obtaining high-quality LNC thin films. Fig. 3 shows XAS spectra for the 80-nm-thick LNC thin film grown at T_s = 600 °C and P_{O2} = 100 mTorr. The Co L_3 edge spectra showed peaks at 780 eV, as shown in Fig. 3(a). This strong absorption originates from the Co $2p_{3/2}$ (L_3) state. This feature indicates that the Co in the film interior was in the Co^{3+} state [20,21]. Additionally, the surface-sensitive TEY spectrum shows that the surface of Co exhibited the same Co^{3+} oxidation state as the interior because the TEY spectrum did not show significant changes compared with the bulk-sensitive transmission spectrum at a photon energy of approximately 780 eV [22].

As expected, the bulk-sensitive transmission-mode spectrum indicates that Ni was in the Ni^{3+} state (Fig. 3(b)). Accordingly, both Co and Ni in the LNC epitaxial thin film showed a formal oxidation state of 3+, consistent with the ideal oxidation state [23]. Note that Ni exhibited a distinct difference in the spectra between the surface and bulk. Fig. 3(b) also shows Ni L_3 edge spectra obtained in the surface-sensitive TEY mode. For the surface-sensitive spectrum, the peak intensity at ~853 eV increased compared to the bulk-sensitive case. The results indicate that Ni is reduced at the surface of the LNC thin film. We speculate that the surface Ni was reduced upon exposure to air [23,24] while transferring the sample to the beamline.

Next, the electrical conductivity of a 40-nm-thick $LiNi_{0.8}Co_{0.2}O_2$ (LNC) epitaxial thin film was measured using the four-probe method. The LNC epitaxial thin film exhibited a conductivity of 0.67 S/cm at 300 K, which was very close to that of a reported bulk sample (approximately 0.3 S/cm) [6].

Finally, we investigated the battery properties and evaluated the solid-electrolyte/electrode interface resistance. After depositing the Li_3PO_4 solid electrolyte and Li-metal negative electrode on LNC epitaxial thin films (T_s = 600 °C and P_{O2} = 100 mTorr), the fabricated thin-film battery [Fig. 4 (a)] was transferred to an electrochemical-property-measurement chamber without exposing the sample to air. Therefore, the surface was free from the reduction caused by air exposure. To the best of our knowledge, while the epitaxial growth of LNC thin films has been reported previously [25], this is the first report on a solid-state battery formed using LNC epitaxial thin films.

Fig. 4 (b) shows the CV curves for the resulting thin-film battery. The voltage was swept at 1 mV s^{-1} in the range between 3.0 and 4.2 V *vs.* Li/Li^+. Oxidative/reductive (Ni^{4+}/Ni^{3+}) current peaks corresponding to the extraction/insertion of Li ions in the LNC were clearly observed at 3.73 and 3.69 V, respectively. The current peaks were sharp and the peak separations between the oxidative/reductive reactions were very small, approximately 0.04 V. Furthermore, the CV curves from the second to the fifth cycles overlapped, indicating superior stability and repeatability in terms of the battery operations. Interestingly, although the crystal orientation of the LNC thin films was unfavorable for ionic transport across the interface between the LNC and Li_3PO_4 electrolyte for the fabricated thin-film batteries, the LNC thin-film batteries exhibited very stable battery operation. We speculated that ions migrated through anti-phase grain boundaries, as illustrated in

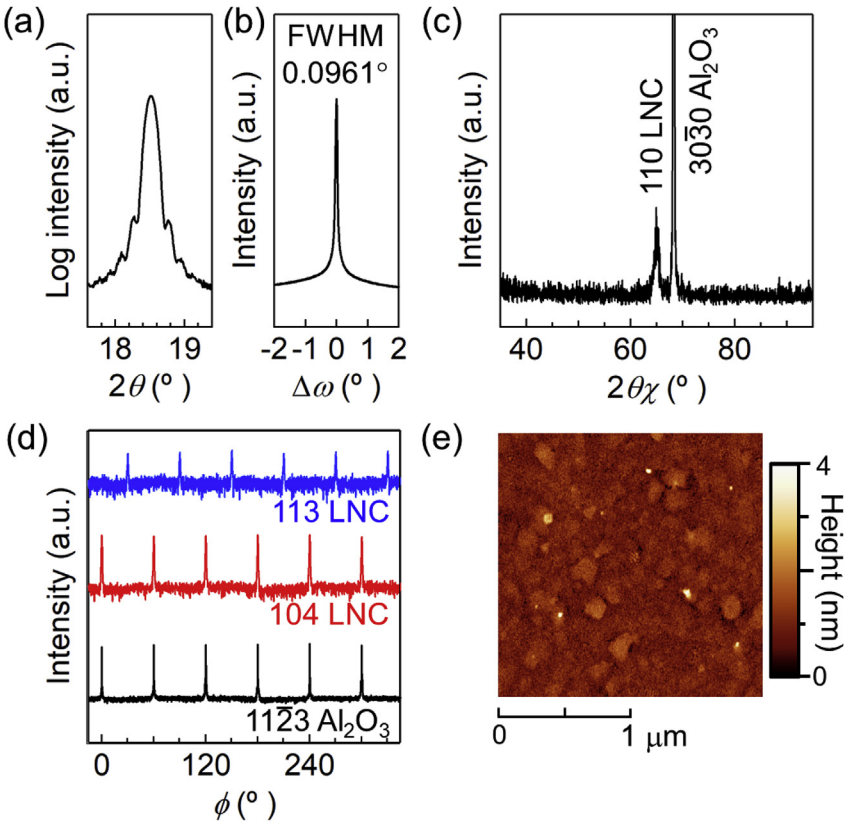

Fig. 2. (a) Out-of-plane X-ray diffraction (XRD) pattern and (b) rocking curve of the 003 reflection for the 50-nm-thick $LiNi_{0.8}Co_{0.2}O_2$ (LNC) thin film. (c) In-plane XRD pattern normal to the Al_2O_3 (10-10) plane. (d) In-plane azimuthal ϕ scans of LNC 113, LNC 104, and Al_2O_3 11–23 reflections. (e) Atomic force microscope image of the 50-nm-thick LNC thin film.

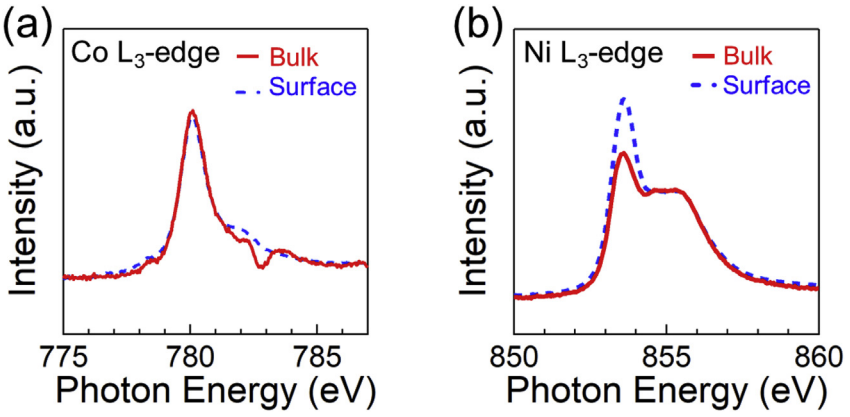

Fig. 3. X-ray absorption spectra obtained using bulk-sensitive transmission mode using X-ray excited optical luminescence from Al_2O_3 substrates and surface-sensitive total-electron-yield mode using the sample drain current. (a) Co L_3 edge and (b) Ni L_3 edge for the $LiNi_{0.8}Co_{0.2}O_2$ epitaxial thin film (80 nm thickness) on the Al_2O_3 (0001) substrate. The peak intensity difference at ~853 eV between the surface and bulk in (b) reflects the difference in the oxidation state of Ni. Note that a dip observed at ~782.5 eV in (a) originated from the effect of Al K-edge absorption of second-order X-rays (~1565 eV).

Fig. 4 (c). It has been reported that anti-phase boundaries with a periodicity of 100–1000 nm are formed at the step edge of Al_2O_3 substrates [19,26]. Therefore, the anti-phase boundaries may serve as ionic conduction paths to the interior of thin films.

Fig. 4 (d) shows the charge/discharge curves in the voltage range of 3.0–4.2 V at a variety of constant currents. A current density of 10 μA cm^{-2} corresponded to a rate of ~3.1C for the thin-film battery. The thin-film battery demonstrated stable operation even at a high rate of 250 μA cm^{-2} (77C) with 30% of the discharge capacity being retained for the rate of 3.1C at room temperature.

The impedance spectra indicate a low resistance at the Li_3PO_4 and LNC interfaces. Fig. 4 (e) shows the impedance spectra for potentials of 3.0 V (discharged state) and 3.8 V (vs. Li+/Li). At 3.0 V, a clear semicircle was observed in the frequency range of 10^3–3×10^5 Hz. Because this semicircle was also observed in the impedance spectrum obtained at 3.8 V, the semicircle probably originated from the impedance of the solid electrolyte, Li_3PO_4. The ionic conductivity of Li_3PO_4 estimated from the impedance spectrum was 3.6×10^{-7} S cm^{-1} (See supporting information), which agrees well with the reported value [27].

As we could not observe a semicircle originating from the Li_3PO_4/LNC interface resistance, it is reasonable to conclude that the interface resistance was very small. Referring to our previous studies regarding $Li_3PO_{4-x}N_x/LiCoO_2$ and $Li_3PO_4/Li(Ni_{0.5}Mn_{1.5})O_4$ interfaces, the semicircle associated with a solid-electrolyte/electrode interface should emerge at approximately 10^3–10^2 Hz [4,5]. These results indicate that the interface resistance was too small to be detected; the semicircle originating from the interface should be much smaller than that originating from Li_3PO_4. We speculated that the interface resistance was less than 7 Ωcm^2. Accordingly, in future work, we intend to employ other solid electrolytes with higher ionic conductivity values or thin solid-electrolyte films to evaluate the resistance of the Li_3PO_4/LNC interface.

4. Conclusion

We demonstrated the stable battery operation of a bottom-current-

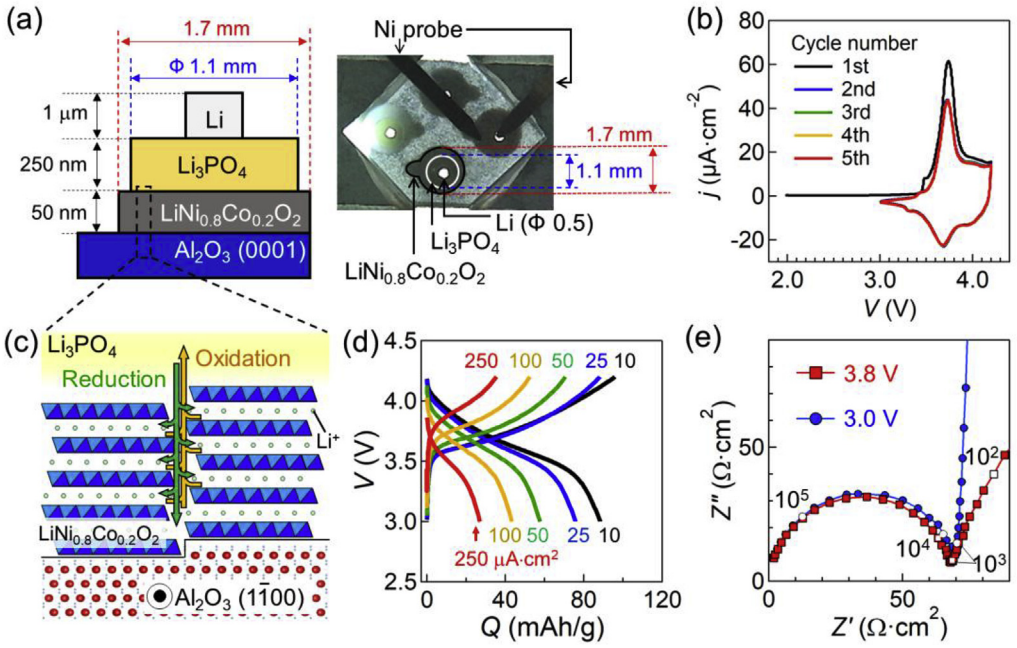

Fig. 4. (a) Schematic cross section (left) and a top-view picture (right) of the fabricated thin-film lithium batteries using $LiNi_{0.8}Co_{0.2}O_2$ (LNC) epitaxial thin films. Note that Ni probing tips are observed. (b) Cyclic voltammogram of the LNC thin-film battery. The sweep rate was 1 mV/s. Note that the second to fifth cycles completely overlapped. (c) Schematic side view of lithium-ion conduction across the interface between LNC and Li_3PO_4. (d) Charge and discharge curves measured at room temperature for the LNC thin-film battery at a variety of current densities. (e) Nyquist plot of impedance spectra at a charging state of 3.8 V (red) and discharged state of 3.0 V (blue). The numbers in the figures indicate the frequencies.

collector-free thin-film battery using highly conductive LNC epitaxial thin films on an Al_2O_3 (0001) substrate. The flatness of the positive electrode was largely improved by eliminating the use of bottom current collectors. The semicircles originating from interface resistance at solid electrolytes and electrodes were too small to be detected. The flat electrode surface is expected to contribute toward understanding the solid-state ionic phenomena at the interfaces of solid electrolytes and positive electrodes.

Acknowledgments

This research was supported by JST-CREST and TOYOTA MOTOR CORPORATION. K. N. acknowledges funding from JSPS Kakenhi Grant no. 17H06674, and no.18K14314. T. H. acknowledges funding from JKA Grant No. 109 and JSPS Kakenhi Grant No. 18H03876. We thank Toray Research Center, Inc. for the RBS-NRA measurements. Raman spectroscopy measurements were performed at Ookayama Materials Analysis Division, Technical Department, Tokyo Institute of Technology.

Appendix A. Supplementary data

Supplementary data to this article can be found online at https://doi.org/10.1016/j.jpowsour.2019.01.067.

References

[1] J.-M. Tarascon, M. Armand, Issues and challenges facing rechargeable lithium batteries, Nature 414 (2001) 359–367.
[2] K. Takada, Progress and prospective of solid-state lithium batteries, Acta Mater. 61 (2013) 759–770 https://doi.org/10.1016/j.actamat.2012.10.034.
[3] N. Ohta, K. Takada, L. Zhang, R. Ma, M. Osada, T. Sasaki, Enhancement of the high-rate capability of solid-state lithium batteries by nanoscale interfacial modification, Adv. Mater. 18 (2006) 2226–2229 https://doi.org/10.1002/adma.200502604.
[4] M. Haruta, S. Shiraki, T. Suzuki, A. Kumatani, T. Ohsawa, Y. Takagi, R. Shimizu, T. Hitosugi, Negligible "negative space-charge layer effects" at oxide electrolyte/electrode interfaces of thin-film batteries, Nano Lett. 15 (2015) 1498–1502 https://doi.org/10.1021/nl5035896.
[5] H. Kawasoko, S. Shiraki, T. Suzuki, R. Shimizu, T. Hitosugi, Extremely low resistance of Li_3PO_4 electrolyte/$Li(Ni_{0.5}Mn_{1.5})O_4$ electrode interfaces, ACS Appl. Mater. Interfaces 10 (2018) 27498–27502 https://doi.org/10.1021/acsami.8b08506.
[6] J. Molenda, P. Wilk, J. Marzec, Transport properties of the $LiNi_{1-y}Co_yO_2$ system, Solid State Ionics 119 (1999) 19–22 https://doi.org/10.1016/S0167-2738(98)00477-9.
[7] M. Haruta, S. Shiraki, T. Ohsawa, T. Suzuki, A. Kumatani, Y. Takagi, R. Shimizu, T. Hitosugi, Preparation and *In-Situ* characterization of well-defined solid electrolyte/electrode interfaces in thin film lithium batteries, Solid State Ionics 285 (2016) 118–121 https://doi.org/10.1016/j.ssi.2015.06.007.
[8] S. Shiraki, H. Oki, Y. Takagi, T. Suzuki, A. Kumatani, R. Shimizu, M. Haruta, T. Ohsawa, Y. Sato, Y. Ikuhara, T. Hitosugi, Fabrication of all-solid-state battery using epitaxial $LiCoO_2$ thin films, J. Power Sources 267 (2014) 881–887 https://doi.org/10.1016/j.jpowsour.2014.05.133.
[9] Nishio, NMC in preparation.
[10] T. Ohnishi, H. Koinuma, M. Lippmaa, Pulsed laser deposition of oxide thin films, Appl. Surf. Sci. 252 (2006) 2466–2471 https://doi.org/10.1016/j.apsusc.2005.04.057.
[11] S. Shiraki, T. Shirasawa, T. Suzki, H. Kawasoko, R. Shimizu, T. Hitosugi, Atomically well-ordered structure at solid electrolyte and electrode interface reduces the interfacial resistance, ACS Appl. Mater. Interfaces 10 (2018) 41732–41737 https://doi.org/10.1021/acsami.8b08926.
[12] A. Rougier, I. Saadoune, P. Gravereau, P. Willmann, C. Delmasa, Effect of cobalt substitution on cationic distribution in $LiNi_{1-y}Co_yO_2$ electrode materials, Solid State Ionics 90 (1996) 83–90 https://doi.org/10.1016/S0167-2738(96)00370-0.
[13] H. Wulff, M.M. Rao, F. Scholz, Crystallographic evidence for the formation of a continuous series of mixed crystals between NiO and $LiNiO_2$, Chem. Mater. 15 (2003) 988–993 https://doi.org/10.1021/cm020584z.
[14] D. Pasero, N. Reeves, L.J. Gillie, A.R. West, Variable oxygen stoichiometry in layered rock salt cathodes, $Li_x(Mn, Ni)O_2$, depending on synthesis conditions, J. Power Sources 174 (2007) 1078–1081 https://doi.org/10.1016/j.jpowersour.2007.06.037.
[15] M.S. Idris, A.R. West, The Effect on cathode performance of oxygen non-stoichiometry and interlayer mixing in layered rock salt $LiNi_{0.8}Mn_{0.1}Co_{0.1}O_{2-\delta}$, J. Electrochem. Soc. 159 (2012) A396–A401 https://doi.org/10.1149/2.039204jes.
[16] R. Kostecki, F. McLarnon, Degradation of $LiNi_{0.8}Co_{0.2}O_2$ cathode surfaces in high-power lithium-ion batteries, Electrochem. Solid State Lett. 5 (2002) A164–A166 https://doi.org/10.1149/1.1482199.
[17] C. Belhomme, M. Cassir, J. Devynck, G. Gregoire, Synthesis by a soft chemistry route and characterization of $Li_xNi_{1-x}O$ ($0 < x < 0.5$) compounds: behavior in molten carbonates, J. Mater. Sci. 35 (2000) 2683–2688 https://doi.org/10.1023/A:1004793607621.
[18] T. Tsuruhama, T. Hitosugi, H. Oki, Y. Hirose, T. Hasegawa, Preparation of layered-rhombohedral $LiCoO_2$ epitaxial thin films using pulsed laser deposition, Appl. Phys. Express 2 (2009) 085502https://doi.org/APEX.2.085502.
[19] S.J. Zheng, C.A.J. Fisher, T. Hitosugi, A. Kumatani, S. Shiraki, Y.H. Ikuhara, A. Kuwabara, H. Moriwake, H. Oki, Y. Ikuhara, Acta Mater. 61 (2013) 7671–7678. Antiphase inversion domains in lithium cobaltite thin films deposited on single-crystal sapphire substrates https://doi.org/10.1016/j.actamat.2013.09.004.
[20] F.M. F de Groot, M. Abbate, J. van Elp, G.A. Sawatzky, Y.J. Ma, C.T. Chen, F. Sette, Oxygen 1s and cobalt 2p X-ray absorption of cobalt oxides, J. Phys. Condens. Matter 5 (1993) 2277–2288 https://doi.org/10.108/0953-8984/5/14/023.
[21] L.A. Montoro, M. Abbate, E.C. Almeida, J.M. Rosolen, Electronic structure of the transition metal ions in $LiCoO_2$, $LiNiO_2$, and $LiCo_{0.5}Ni_{0.5}O_2$, Chem. Phys. Lett. 309 (1999) 14–18 https://doi.org/10.1016/S0009-2614(99)00650-8.
[22] C. Yogi, D. Takamatsu, K. Yamanaka, H. Arai, Y. Uchimoto, K. Kojima, I. Watanabe, T. Ohta, Z. Ogumi, Soft X-ray absorption spectroscopic studies with different probing depths: effect of an electrolyte additive on electrode surfaces, J. Power Sources 248 (2014) 994–999 https://doi.org/10.1016/j.jpowsour.2013.10.030.

[23] Z.W. L-Higgins, S. Sallis, N.V. Faenza, F. Badway, N. Pereira, D.M. Halat, M. Wahila, C. Schlueter, T.-L. Lee, W. Yang, C.P. Grey, G.G. Amatucci, L.F.J. Piper, Evolution of the electrode-electrolyte interface of $LiNi_{0.8}Co_{0.15}Al_{0.05}O_2$ electrodes due to electrochemical and thermal stress, Chem. Mater. 30 (2018) 958–969 https://doi.org/10.1021/acs.chemmater.7b04782.

[24] I.A. Shkrob, J.A. Gillbert, P.J. Phillips, R. Klie, R.T. Haasch, J. Bareño, D.P. Abraham, Chemical weathering of layered Ni-rich oxide electrode materials: evidence for cation exchange, J. Electrochem. Soc. 164 (2017) A1489–A1498 https://doi.org/10.1149/2.0861707jes.

[25] M. Hirayama, K. Sakamoto, T. Hiraide, D. Mori, A. Yamada, R. Kaano, N. Sonoyama, K. Tamura, J. Mizuki, Characterization of electrode/electrolyte interface using in situ X-ray reflectometry and $LiNi_{0.8}Co_{0.2}O_2$ epitaxial film electrode synthesized by pulsed laser deposition method, Electrochim. Acta 53 (2007) 871–881 https://doi.org/10.1016/j.electacta.2007.07.074.

[26] H. Moriwake, A. Kuwabara, C.A.J. Fisher, R. Huang, T. Hitosugi, Y.H. Ikuhara, H. Oki, Y. Ikuhara, First-principles calculations of lithium-ion migration at a coherent grain boundary in a cathode material, $LiCoO_2$, Adv. Mater. 25 (2013) 618–622 https://doi.org/10.1002/adma.201202805.

[27] N. Kuwata, N. Iwagami, Y. Tanji, Y. Matsuda, J. Kawamura, Characterization of Thin-film lithium batteries with stable thin-film Li_3PO_4 solid electrolytes fabricated by ArF excimer laser deposition, J. Electrochem. Soc. 157 (2010) A521–A527 https://doi.org/10.1149/1.3306339.